**JASS 2008**

# SIMULATION OF THE FIRE EXTINGUISHMENT PROCESS BY FINE WATER SPRAY

Lipjainen Alexei
Saint-Petersburg State Polytechnic University
Email: alex_ykka@mail.ru
ICQ 196198342

## ABSTRACT

Rapidly growing technology of fire suppression by high-pressure fine water sprays exploits its capability to mitigate gaseous flame faster with smaller water flow rate, yet applying environmentally friendly and toxically safe extinguishing agent. For the optimum use of water in fire suppression, two contradictory requirements should be met: efficient delivery of the dispersed water into the flame zone and rapid droplet evaporation. This work aims to develop the appropriate mathematical model of a turbulent evaporating spray, to incorporate the model into the existing in-house Fire3D software, and to investigate numerically the interaction of fine and coarse water sprays with buoyant turbulent diffusion flame. As a result, the mechanisms of spray-flame interaction are identified, and the drastic differences between the coarse and fine water sprays are demonstrated. Both symmetric (spray nozzle at the flame axis, the spray is directed downwards) and asymmetric (spray nozzle away from the flame axis, the spray is inclined towards the flame) are considered.

## 1. INTRODUCTION

Development of fixed water mist fire suppression systems offers an alternative to halons prohibited by the Montreal protocol. It also provides an opportunity to obey challenging new requirements of the international safety standards. However, for the optimum use of water in fire suppression, two contradictory requirements should be met: efficient delivery of the dispersed water into the flame zone and rapid droplet evaporation. Furthermore, an optimum solution cannot be universal since it depends on a possible fire scenario, geometry of the protected compartment, ventilation conditions, among others. That inspires massive computer simulations requiring a robust mathematical model. Despite the intensive research activities worldwide, robust modeling and simulations of fine evaporating spray in turbulent flame extinguishment remains a challenging task yet to be resolved. Also, turbulent spray dynamics and the spray-flame interaction mechanisms may be qualitatively different depending on the initial droplet size distribution; very fine spray (or mist) performance, although promising, calls for further investigations.

## 2. MODEL DESCRIPTION

### 2.1. Gas phase modeling

The model of the gas phase is the Navier-Stokes equation system for the multicomponent reacting mixture. In this work, URANS simulations are performed by solving Favre-averaged component, momentum and enthalpy transport equations. Modified $k$-ε model is used to predict mean turbulent fields. Primary modification introduced in the model is correction to the generation term in the dissipation equation that makes it sensitive to axial mean velocity distribution in a rising buoyant flow. Such a correction significantly improves predictions of flow characteristics in axially symmetric buoyant flames. The low Mach number flow is considered for which the gas density is determined by the ideal gas state equation at a constant atmospheric pressure. The solution that obeys both discretized momentum equation and continuity equation is obtained by a fractional-step projection method. An irreversible single-step reaction is assumed for fuel (methane) oxidation, and the burning rate is

determined by the eddy break-up model. Radiative heat transfer has been simulated by the Monte-Carlo method. Total absorption coefficient for the mixture of water vapor, carbon dioxide and soot was calculated via the total emissivity obtained by the weighted-sum-of-gray-gases model.

Transport equations were discretized by the finite volume technique using non-uniform structured Cartesian grids. After solving gas phase transport equations, the evaporating droplet spray parameters were calculated to determine the source terms, corresponding to the two-way interphase exchange by mass (due to droplet evaporation), momentum (due to drag), and enthalpy (due to heating or cooling of droplets).

### 2.2. Liquid phase modeling

A Lagrangian approach is applied to model evaporating spray. Given the gas flow characteristics, multiple discrete droplets are tracked along their trajectories. Droplet velocity may change due to the gravity and drag forces, while the effects of Basset force, Saffman lift force, Magnus force, and of the virtual-mass term have been neglected due to considerable disparity in gas and liquid densities. To make computations feasible, the momentum (as well as mass and energy) conservation equation is considered for a group of similar droplets (called as *particle* hereafter). For velocity and location of every particle, the following equations are solved:

$$\frac{du_{p,i}}{dt} = -\left(\frac{3\bar{\rho}C_D}{4d_p\rho_p}\right)|u_{p,i}-\tilde{u}_i|(u_{p,i}-\tilde{u}_i)+g_i\left(1-\frac{\bar{\rho}}{\rho_p}\right) \qquad \frac{dx_{p,i}}{dt}=u_{p,i}, \qquad (1)$$

where $\tilde{u}_i$ and $u_{p,i}$ are the mean gas and particle velocity components, $\rho$ and $\rho_p$ are the gas and droplet densities, and $d_p$ is the droplet diameter. The drag coefficient is obtained as

$$C_D = \begin{cases} 24/\mathrm{Re}_p(1+0.15\mathrm{Re}_p^{2/3}) & ,\mathrm{Re}_p<1000 \\ 0.44 & ,\mathrm{Re}_p>1000 \end{cases}, \qquad (2)$$

where $\mathrm{Re}_p = d_p|\tilde{\vec{u}}-\vec{u}_p|/\nu$ is the particle Reynolds number.

Turbulent dispersion may have a considerable effect, particularly for fine droplets. To take such an effect into account, the carrying phase velocity, $\tilde{u}_i+u_i'$, is decomposed to the sum of the mean value $\tilde{u}_i$ (which is determined from momentum equation) and the stochastic component, $u_i'$, which is statistically modeled by Monte-Carlo approach. We suppose that eddies have the mean velocity fluctuations $\sqrt{2k/3}$, the mean size $l_t = C_\mu^{3/4}k^{3/2}/\varepsilon$ and the lifetime $\tau_t = l_t/\sqrt{2k/3}$. Assuming the mean gas velocity and the droplet dynamic relaxation time $\tau_D$

$$\tau_D = \frac{4d_p\rho_p}{3\rho C_D|\tilde{\vec{u}}-\vec{u}_p|} \qquad (3)$$

to be constant along the distance of $l_t$, the droplet transit time for the above distance is

$$\tau_p = \begin{cases} -\tau_D\ln\left(1-\dfrac{l_t}{\tau_D|\vec{u}_p-\vec{u}_p^*|}\right) & ,\text{if } l_t<\tau_D|\vec{u}_p-\vec{u}_p^*| \\ \infty & ,\text{if } l_t>\tau_D|\vec{u}_p-\vec{u}_p^*| \end{cases}, \qquad u_{p,i}^* = \tilde{u}_i+\tau_D g_i(1-\rho/\rho_p), \qquad (4)$$

The time of interaction of the particle with the eddy is therefore $\tau_{p,t} = \min(\tau_p,\tau_t)$.

In Eq. (1), the perturbed velocity $\tilde{u}_i+u_i'$ is substituted instead of mean velocity $\tilde{u}_i$, where the fluctuation velocity $u_i'$ is randomly sampled using the zero-centered Gaussian distribution with the

standard deviation of $\sigma = \sqrt{2k/3}$. Next value of $u_i'$ is sampled as soon as the particle-eddy interaction time $\tau_{p,t}$ is expired.

Particle temperature is changed due to the heat transfer from and to the carrying gas and due to the droplet evaporation:

$$m_p C_{p,l} \frac{dT_p}{dt} = \begin{cases} q_{p,conv} + \Delta h_{vap}(T_p) \dfrac{dm_p}{dt} & ,T_p < T_{boil} \\ 0 & ,T_p = T_{boil} \end{cases}, \tag{5}$$

where $C_{p,l}$ is the droplet specific heat, and $\Delta h_{vap}(T_p) = \Delta h_{vap,boil} + \int_{T_p}^{T_{boil}} C_{p,l}(T)dT$ is the latent heat of liquid evaporation at droplet temperature. The convective heat flux is

$$q_{p,conv} = -\pi d_p \mathrm{Nu} \frac{\mu_g}{\mathrm{Pr}} C_{P,g}\left(T_p - \tilde{T}\right), \tag{6}$$

where $\mathrm{Nu} = 2 + 0.6\,\mathrm{Re}_p^{1/2}\,\mathrm{Pr}^{1/3}$ is the Nusselt number, $\mu_g$ and $C_{P,g}$ are the gas viscosity and specific heat.

Droplet mass loss rate is determined by the rate of vapor diffusion away from the droplet surface (when droplet temperature is below the boiling point) or by the rate of heat transfer (when the droplet temperature equals the boiling point). That is reflected by the droplet mass balance equation:

$$\frac{dm_p}{dt} = \begin{cases} -\pi d_p \mu_g \dfrac{\mathrm{Sh}}{\mathrm{Pr}} \ln(1 + B_m) & ,T_p < T_{boil} \\ -\dfrac{q_{p,conv}}{\Delta h_{vap}(T_{boil})} & ,T_p = T_{boil} \end{cases}, \tag{7}$$

where $\mathrm{Sh} = 2 + 0.6\,\mathrm{Re}_p^{1/2}\,\mathrm{Sc}^{1/3}$ is the Sherwood number, $B_m = \left(Y_{vap,sat}(T_p) - Y_{vap,\infty}\right) / \left(1 - Y_{vap,sat}(T_p)\right)$ is the Spalding number, $Y_{vap,sat}(T_p)$ is the saturated vapor mass fraction at droplet temperature, $Y_{vap,\infty}$ is the vapor mass fraction in the carrying gas (note that the water vapor is also produced in combustion), and $T_{boil}$ is the boiling temperature. Droplet mass is kept unchanged when $Y_{vap,sat}(T_p) < Y_{vap,\infty}$.

The gas-droplet coupling terms (source terms in continuity, momentum and energy equations) are calculated in such way (8)-(10), and then assigned to the center of every control volume:

$$\dot{\bar{r}}_M = -\sum \frac{n_p}{\Delta V} \frac{dm_p}{dt}, \tag{8}$$

$$\dot{\bar{r}}_V = -\sum \frac{n_p}{\Delta V} \left( m_p \frac{\vec{u}_p - \tilde{\vec{u}}}{\tau_D} - \vec{u}_p \frac{dm_p}{dt} \right), \tag{9}$$

$$\dot{\bar{r}}_H = -\sum \frac{n_p}{\Delta V} \left( m_p C_p \frac{T_p - \tilde{T}}{\tau_T} - h_{vap}(T_p) \frac{dm_p}{dt} \right), \tag{10}$$

where $n_p$ is the number of real droplets per particle, $h_{vap}(T_p)$ is the vapor enthalpy at droplet temperature. In Eqs. (8), (9), (10), summation is performed over all the particles in a given control volume. The values of $\dot{\bar{r}}_M$, $\dot{\bar{r}}_V$ and $\dot{\bar{r}}_H$ are then used to solve continuity, momentum and energy equations for gas phase at the next time step.

### 2.3. Modeling sprinkler spray

Modeling the sprinkler spray implies determination of initial droplet velocity magnitude and direction, diameter and temperature of the discharged liquid when it exhausts through the nozzle being

subsequently atomized. The sprinkler is modeled here as a point source of droplets having velocity vectors uniformly distributed inside the cone of angle $\varphi$.

To allow for the droplet polydispersity, the Rosin-Rammler distribution is used:

$$R(d_p) = \exp\left(-\ln 2\left(\frac{d_p}{d_{50}}\right)^{\gamma}\right), \qquad (11)$$

where $R(d_p)$ is the accumulated mass of droplets having diameters greater than $d_p$. Given the spread parameter $\gamma$, the median droplet diameters $d_{50}$ characterizes the initial spray dispersion (note that $R(d_{50})$ = 0.5). For the spread parameter the constant value of $\gamma$ = 2.4 was used.

## 3. RESULTS AND DISCUSSION

In the simulations, the experimental conditions were replicated where the water spray suppressed the buoyant turbulent diffusion flame. The flame was produced by the methane-fuelled burner with the exit surface (18 cm diameter) located at the floor level. Fuel flow rate corresponds to the flame calorific power of $\dot{Q}$ = 15 kW. For more information about experiment see article [1]. Two nozzle locations and cone orientations are considered and compared. In the first scenario (*symmetric spray*), the nozzle is located at the vertical flame axis (at the level of 1.6 m) and the spray axis is directed downward – all conditions are similar to [1]. In the second one (*asymmetric spray*), the nozzle is located 0.5 m away from the vertical flame axis, and the spray axis is inclined towards the flame.

The simulation methodology includes three stages.

The first one is the transient simulation of the gas flame in the open space above the burner until steady state (without spray). The results are then used as initial conditions for the third stage - simulation of the fire extinguishment process by fine water spray. The simulations have been performed in 3×3×3 m computational domain. On this stage we made a comparison with experimental data from [2] – Fig. 1.

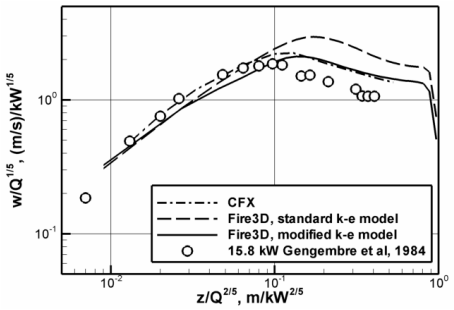


Figure 1. Mean velocity distributions along the flow axis

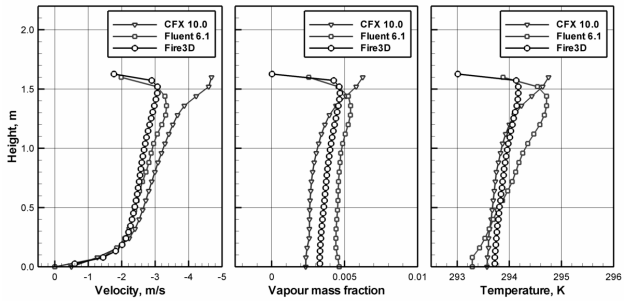


Figure 2. Spray simulations with three CFD codes

Stage two – modeling of symmetric spray without flame. Detailed measurements for validation of spray model are lacking. Due to that, a comparison was made here between the predictions by three CFD codes (Fire3D, Ansys CFX 10.0 and Ansys Fluent 6.1) to verify their performance for the same benchmark problem: water flow rate is 7.57 l/min, initial droplet size equal to 0.500 mm (monodisperse distribution), initial droplet temperature 298 K, ambient air temperature 293 K. Geometry of the domain and location of the nozzle were discussed above. Comparisons are shown in Fig. 2. Despite a considerable discrepancy, all three codes produce qualitatively similar data, Fire3D results being between the other two.

The third stage is **simulation of the fire extinguishment process by fine water spray.**

It was found that the decrease in the initial droplet diameter drastically changes the spray dynamics and the mode of its interaction with flame:

- The estimates show that 630μ initial diameter (*coarse spray*) and 15 m/s initial velocity droplets retain their momentum up to a distance of 2 m while their 80μ (*fine spray*) counterparts lose its momentum at a distance of an order of magnitude less. The carrying gas flow itself is formed by the coarse spray and is directly affected by the spray momentum
- The shape of the *coarse* spray is determined by the initial spray spreading angle, and, alternatively, *fine* water spray is of much smaller diameter which is controlled by the toroidal large-scale vortex surrounding the spray and creating the entraining gas flow.
- The simulation results indicate that for the same flow rates and droplet velocity distributions (velocity magnitude and cone shape), finer spray suppresses flame more rapidly than the coarse one. This is illustrated by Fig. 3 *a*, where the predicted maximum value of the mean flame temperature is shown as a function of time. One of the reasons for such a remarkable difference is shown in Fig. 3 *b*, which demonstrates the rate of vapor generation upon spray evaporation. The fine spray produces the amount of vapor which is by more than an order of magnitude greater than that produced by the coarse spray.

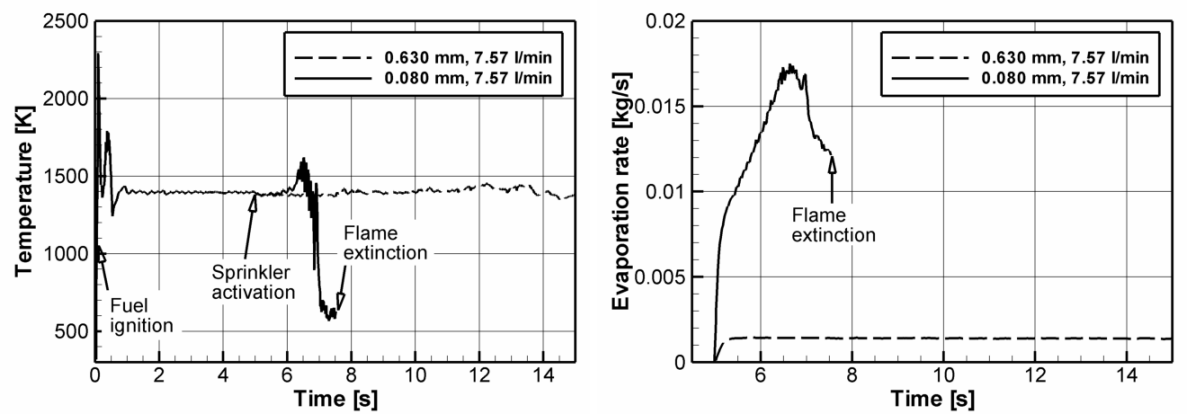


(a) (b)

Figure 3. The effect of initial spray dispersion on transient spray-flame interaction: *a* – mean flame temperature (maximum value); *b* – spray evaporation rate

- It has also been found that in the coarse spray case evaporated fraction (portion of the evaporated mass per unit time in the total water flow rate) is about 1% regardless of the flow rate. It means that vast majority of water is transported to the solid walls rather than evaporated to affect the gas flame. Fig. 4 *a* - proportionality of the evaporation rate to the nozzle flow rate. Alternatively, in the fine spray the evaporated fraction varies from 15 to 30%, and the increase of the flow rate causes observable decrease in the evaporated fraction although absolute value of the evaporation rate increases (Fig. 4 *b*).

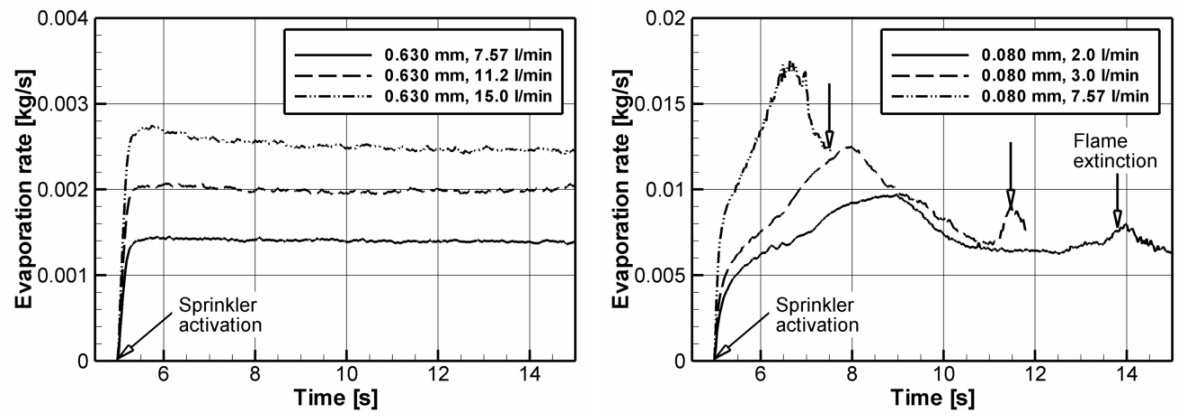


(a) (b)

Figure 4. Transient spray evaporation rate: *a* – coarse spray; *b* – fine spray

- It is very important that the large droplets easily penetrate into the flaming region where its evaporation rate increases thereby creating local maximum of vapor concentration *inside* the

flame. Alternatively, fine droplets cannot penetrate inside the flame being deflected by the gas flow. Instead, they form the vapor cloud that surrounds the flame from the *outside*. This explains why fine water spray (mist) is most suitable as a total flooding agent in closed compartments where gas flame mitigation is a primary target of fire suppression.

One of the major results is that the symmetric coarse spray destabilizes flame but does not extinguish it for a rather long time, while the *symmetric fine spray suppresses the flame in a few seconds*, Fig. 5 *a,b*.

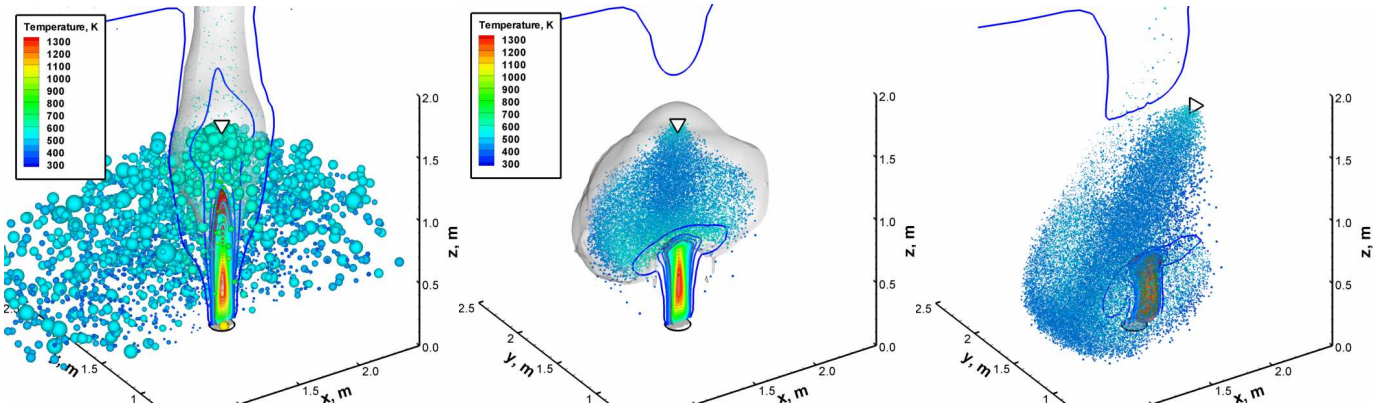


(a) 17 sec (b) 1 sec (c) 1 sec

Figure 5. Flame suppression by symmetric and asymmetric water sprays (water flow rate is 7.57 l/min): *a* - coarse spray, initial median droplet diameter 0.630 mm (17 s after nozzle activation); *b*, *c* - fine sprays, initial median droplet diameter 0.080 mm (1.0 s after nozzle activation). Transparent surface shows 0.2% volume fraction of vaporized water.

A series of simulations has been performed for the asymmetric nozzle location and inclined spray axis direction (asymmetric sprays). It was found that due to greater flame cross-section area attacked by the spray, the asymmetric spray affects the flame much stronger than its symmetric counterpart, Fig. 5 *c*. In the case of *fine spray* the flame can be deflected not only by its central core propagating downstream but also by the secondary vertical flow in the opposite direction. This leads to faster suppression than in the case of symmetric spray with the same water flow rate.

## CONCLUSIONS

The model is presented of the evaporating spray that affects the buoyant turbulent diffusion flame. Better understanding of physics and ability to accurately predict the spray-flame interaction is sought, with the ultimate aim to contribute into design of the efficient and environmentally friendly halon-free fire suppression methodology.

The model is incorporated into the existing CFD software Fire3D and applied to predict the effect of the initial droplet size distribution on the spray-flame interaction. Two distinct mechanisms of flame mitigation are demonstrated when coarse and fine sprays were considered. Simulation results have shown that in the fire scenario considered, fine water spray causes faster flame extinguishment with smaller water flow rate.

It can also be concluded that these model requires further development – implementation of large eddy simulation methodology, consideration of droplet-droplet interaction, flame extinction modeling. At current time our work is focused on development of multiprocessor version of in-house software.

## REFERENCES


1. Schwille J.A., Lueptow R.M. (2006) The reaction of a fire plume to a droplet spray // Fire Safety Journal, Vol. 41, 2006, 390–398.
2. Gengembre E., Cambray P., Karmed D., Bellet J. C. Turbulent diffusion flames with large buoyancy effects // Combustion Science and Technology, Vol. 41, 1984, 55-67.